

# Extending INLA to a class of near-Gaussian latent models

Thiago G. Martins and Håvard Rue

Department of Mathematical Sciences

Norwegian University of Science and Technology

N-7491 Trondheim, Norway

January 16, 2021

## Abstract

This work extends the Integrated Nested Laplace Approximation (INLA) method to latent models outside the scope of latent Gaussian models, where independent components of the latent field can have a near-Gaussian distribution. The proposed methodology is an essential component of a bigger project that aim to extend the R package INLA (R-INLA) in order to allow the user to add flexibility and challenge the Gaussian assumptions of some of the model components in a straightforward and intuitive way. Our approach is applied to two examples and the results are compared with that obtained by Markov Chain Monte Carlo (MCMC), showing similar accuracy with only a small fraction of computational time. Implementation of the proposed extension is available in the R-INLA package.

**Keywords:** Approximate Bayesian inference, INLA, MCMC, near-Gaussian latent models

## 1 Introduction

Integrated Nested Laplace Approximation (INLA) is an approach proposed by Rue et al. (2009) to perform approximate fully Bayesian inference on the class of latent Gaussian models (LGM). It was demonstrated in the original paper that, when compared with the more usual Markov Chain Monte Carlo (MCMC) schemes (Robert and Casella, 2004; Gamerman and Lopes, 2006), INLA outperforms the latter both in terms of accuracy and speed. Monte Carlo averages under MCMC are characterized by additive  $O_p(N^{-1/2})$  errors, where  $N$  is the simulated sample size, meaning that we need 100 times more computational time to improve our estimates by one digit. Besides that, due to the additive nature of Monte Carlo estimates, it is even harder to accurately estimate tail probabilities with MCMC. On the other hand, INLA bypasses the need

for stochastic simulation by an extensive use of simple and fast Gaussian approximations to take advantage of the properties of latent Gaussian models, where for most real problems and data sets, the conditional posterior of the latent field is typically well behaved, being close to a Gaussian. As opposed to MCMC, INLA has relative error which allow for more accurate estimates of small quantities, as for example the estimation of tail probabilities.

INLA is not meant to be a replacement of MCMC in applied statistics, but it is a specific tailored algorithm that works extremely well in the broad class of LGMs, and thus offers a better option in this context. Given the wide range of models that belong to the class of LGMs, it is common to start our analysis with some standard model  $M_0$ , contained within the LGM class, to solve a particular set of problems. However, we sometimes realize that our analysis would be compromised if the data has specific deviations from the modeling assumptions in  $M_0$ . A natural way to robustify  $M_0$  against these deviations is to embed it into a larger, more flexible model  $M_1$  (Box, 1980), possibly outside the realm of LGMs. To give a more specific example, assume we start with a simple linear mixed effects model (Laird and Ware, 1982) with a Gaussian random effect. It is well known in the literature that the Gaussian distribution is not robust against outliers (Lange et al., 1989), and a sensible approach would be to embed our model into a larger model that is robust to outliers. One example is the model proposed by Pinheiro et al. (2001), where Student's  $t$  distributions are used for both the error terms and the random effects. Unfortunately, although the current implementation of INLA can deal with non-Gaussian likelihoods, it cannot handle non-Gaussian latent components, as the Student's  $t$  random effects in this example.

This paper proposes an extension that allows INLA to be applied to models where some independent components of the latent field have a non-Gaussian distribution. Interest for such models arise often in the literature but the lack of user friendly software able to handle them in a fast and accurate way might lead someone to stay with more standard models, even though it might not be the best for their applications. This proposed extension is an essential component of a bigger project that aim to extend the R package INLA (R-INLA) in order to allow the user to add flexibility and to challenge the Gaussian assumptions of some of the model components in a straightforward and intuitive way. Specifically, we plan to give an option in R-INLA for the user that start with a initial model  $M_0$  based on Gaussian distributions to expand the model in certain directions by adding flexibility around these Gaussian distributions, e.g. correcting it for asymmetry and/or kurtosis. We refer to these distributions that add flexibility around the Gaussian as *near-Gaussian distributions*, as will be explained in Section 3.1. But for this to be accomplished we need the methodology presented in this paper to be able to perform inference

in these near-Gaussian latent models.

Besides being an essential component of the model expansion feature described above, the approach presented here is useful in itself, since it allows us to fit models that are currently in demand and lie outside the LGM framework. Examples of such models are survival models with gamma frailty (Ibrahim et al., 2001) where the random effects have a log gamma distribution, the already mentioned robust mixed effect models (Pinheiro et al., 2001), where the distribution of the random effects is assumed to be Student's  $t$  rather than Gaussian, thus allowing for outlier identification and accommodation and non-Gaussian state space models (Kitagawa, 1987), where the distribution of the noise in the state space evolution equation is assumed to be non-Gaussian. The list is, of course, much longer than that, and a reliable method to fit this large class of models efficiently will provide the right tools for the applied scientist to practice a more flexible and realistic data analysis.

Our extension is not straightforward given the central role that the latent Gaussian field plays in the INLA methodology. In this paper, we take advantage of the types of approximations performed and the way they are combined in INLA to propose a new way to look at this latent near-Gaussian models of interest and show how to adapt INLA to fit this more complex class of models. The paper is organized as following: Section 2 will describe the latent Gaussian models and the INLA methodology, highlighting the importance of the Gaussian latent field to the success of the method. Section 3 defines the sub-class of latent models of interest in this paper and describes our proposed extension to fit this set of models. Section 4 illustrates our approach with two examples and Section 5 offers a conclusion. The proposed extension is already implemented as part of the R package INLA, and its use is illustrated in Appendix A, where the R code from the example in Section 4.1 is displayed. <sup>1</sup>

## 2 Integrated Nested Laplace Approximation

This section contains a brief description of latent Gaussian models and a review of the INLA method proposed by Rue et al. (2009). Latent Gaussian models have a wide range of applications including, for example, regression models, dynamic models, spatial and spatiotemporal models. In Section 2.1 we define the class of latent Gaussian models and its hierarchical representation that will make the exposition of the approximation methods described in this paper easier to read. The Gaussian approximation to conditional distributions of the latent Gaussian field, which is the core of INLA is described in Section 2.2. The INLA method applied to latent

---

<sup>1</sup>Please visit <http://www.r-inla.org/> for more information about the R package INLA.

Gaussian models is described in Section 2.3, while the importance of the Gaussian prior on the latent field to the success of INLA is made explicit in Section 2.4.

## 2.1 Latent Gaussian models

The INLA framework was designed to deal with latent Gaussian models where the observation (or response) variable  $y_i$  is assumed to belong to a distribution family (not necessarily part of the exponential family) where some parameter of the family  $\phi_i$  is linked to a structured additive predictor  $\eta_i$  through a link function  $g(\cdot)$ , so that  $g(\phi_i) = \eta_i$ . The structured additive predictor  $\eta_i$  accounts for effects of various covariates in an additive way:

$$\eta_i = \alpha + \sum_{j=1}^{n_f} f^{(j)}(u_{ji}) + \sum_{k=1}^{n_\beta} \beta_k z_{ki} + \epsilon_i, \quad (1)$$

where  $\{f^{(j)}(\cdot)\}$ 's are unknown functions of the covariates  $\mathbf{u}$ , used for example to relax linear relationship of covariates and to model temporal and/or spatial dependence, the  $\{\beta_k\}$ 's represent the linear effect of covariates  $\mathbf{z}$  and the  $\{\epsilon_i\}$ 's are unstructured terms. Then a Gaussian prior is assigned to  $\alpha$ ,  $\{f^{(j)}(\cdot)\}$ ,  $\{\beta_k\}$  and  $\{\epsilon_i\}$ .

We can also write the model described above using a hierarchical structure, where the first stage is formed by the likelihood function with conditional independence properties given the latent field  $\mathbf{x} = (\boldsymbol{\eta}, \alpha, \mathbf{f}, \boldsymbol{\beta})$  and possible hyperparameters  $\boldsymbol{\theta}_1$ , where each data point  $\{y_i, i = 1, \dots, n_d\}$  is connected to one element in the latent field  $x_i$ . Assuming that the elements of the latent field connected to the data points are positioned on the first  $n_d$  elements of  $\mathbf{x}$ , we have

$$\text{Stage 1. } \mathbf{y}|\mathbf{x}, \boldsymbol{\theta}_1 \sim \pi(\mathbf{y}|\mathbf{x}, \boldsymbol{\theta}_1) = \prod_{i=1}^{n_d} \pi(y_i|x_i, \boldsymbol{\theta}_1).$$

Note that the linear predictor  $\boldsymbol{\eta}$  are usually the first  $n_d$  elements of  $\mathbf{x}$ , as represented by the notation  $\mathbf{x} = (\boldsymbol{\eta}, \alpha, \mathbf{f}, \boldsymbol{\beta})$  used before. The reason to include the linear predictors in the latent field is purely computational as it allows the INLA software to be coded for LGMs in general and not on a case-by-case basis.

The conditional distribution of the latent field  $\mathbf{x}$  given some possible hyperparameters  $\boldsymbol{\theta}_2$  forms the second stage of the model and has a joint Gaussian distribution,

$$\text{Stage 2. } \mathbf{x}|\boldsymbol{\theta}_2 \sim \pi(\mathbf{x}|\boldsymbol{\theta}_2) = \mathcal{N}(\mathbf{x}; \boldsymbol{\mu}(\boldsymbol{\theta}_2), \mathbf{Q}^{-1}(\boldsymbol{\theta}_2)),$$

where  $\mathcal{N}(\cdot; \boldsymbol{\mu}, \mathbf{Q}^{-1})$  denotes a multivariate Gaussian distribution with mean vector  $\boldsymbol{\mu}$  and a precision matrix  $\mathbf{Q}$ . In most applications, the latent Gaussian field have conditional independence properties, which translates into a sparse precision matrix  $\mathbf{Q}(\boldsymbol{\theta}_2)$ , which is of extreme importance for the numerical algorithms that will follow. The latent field  $\mathbf{x}$  may have additional linear

constraints of the form  $\mathbf{A}\mathbf{x} = \mathbf{e}$  for an  $k \times n$  matrix  $\mathbf{A}$  of rank  $k$ , where  $k$  is the number of constraints and  $n$  the size of the latent field. The hierarchical model is then completed with an appropriate prior distribution for the hyperparameters of the model  $\boldsymbol{\theta} = (\boldsymbol{\theta}_1, \boldsymbol{\theta}_2)$

**Stage 3.**  $\boldsymbol{\theta} \sim \pi(\boldsymbol{\theta})$ .

## 2.2 The Gaussian approximation

The Gaussian approximation to densities of the form

$$\pi(\mathbf{x}|\boldsymbol{\theta}, \mathbf{y}) \propto \exp \left\{ -\frac{1}{2} \mathbf{x}^T \mathbf{Q}(\boldsymbol{\theta}) \mathbf{x} + \sum_{i \in I} g_i(x_i) \right\}, \quad (2)$$

plays a important role in INLA, where  $g_i(x_i)$  is a function of  $x_i$  that may depend on  $y_i$  and  $\boldsymbol{\theta}$ , and  $I$  is an index set. Hence in this section we describe one of the many possible ways to approximate (2) by a Gaussian distribution.

We can perform a Taylor expansion up to second order of  $g_i(x_i)$  around an initial guess  $\mu_i^{(0)}$

$$g_i(x_i) \approx g_i(\mu_i^{(0)}) + b_i x_i - \frac{1}{2} c_i x_i^2,$$

where  $b_i$  and  $c_i$  depend on  $\mu_i^{(0)}$ , and then a Gaussian approximation is obtained with precision matrix  $\mathbf{Q} + \text{diag}(\mathbf{c})$  and mode given by the solution of  $\{\mathbf{Q} + \text{diag}(\mathbf{c})\} \boldsymbol{\mu}^{(1)} = \mathbf{b}$ , where  $\mathbf{b}$  and  $\mathbf{c}$  are vectors formed by  $b_i$ 's and  $c_i$ 's respectively. This process is repeated until it converges to a Gaussian distribution with, say, mean  $\boldsymbol{\mu}^*$  and precision matrix  $\mathbf{Q}^* = \mathbf{Q} + \text{diag}(\mathbf{c}^*)$ , where  $\mathbf{c}^* = \mathbf{c}(\boldsymbol{\mu}^*)$ , which we denote hereafter by  $\pi_G(\mathbf{x}|\boldsymbol{\theta}, \mathbf{y})$ .

## 2.3 The INLA method

For the hierarchical model described in Section 2.1 the joint posterior distribution of the unknowns then reads

$$\begin{aligned} \pi(\mathbf{x}, \boldsymbol{\theta}|\mathbf{y}) &\propto \pi(\boldsymbol{\theta}) \pi(\mathbf{x}|\boldsymbol{\theta}) \prod_{i=1}^{n_d} \pi(y_i|x_i, \boldsymbol{\theta}) \\ &\propto \pi(\boldsymbol{\theta}) |\mathbf{Q}(\boldsymbol{\theta})|^{n/2} \exp \left[ -\frac{1}{2} \mathbf{x}^T \mathbf{Q}(\boldsymbol{\theta}) \mathbf{x} + \sum_{i=1}^{n_d} \log\{\pi(y_i|x_i, \boldsymbol{\theta})\} \right] \end{aligned}$$

The approximated posterior marginals of interest  $\tilde{\pi}(x_i|\mathbf{y})$ ,  $i = 1, \dots, n$  and  $\tilde{\pi}(\theta_j|\mathbf{y})$ ,  $j = 1, \dots, m$  returned by INLA has the following form

$$\tilde{\pi}(x_i|\mathbf{y}) = \sum_k \tilde{\pi}(x_i|\boldsymbol{\theta}^{(k)}, \mathbf{y}) \tilde{\pi}(\boldsymbol{\theta}^{(k)}|\mathbf{y}) \Delta \boldsymbol{\theta}^{(k)} \quad (3)$$

$$\tilde{\pi}(\theta_j|\mathbf{y}) = \int \tilde{\pi}(\boldsymbol{\theta}|\mathbf{y}) d\boldsymbol{\theta}_{-j} \quad (4)$$

where  $\{\tilde{\pi}(\boldsymbol{\theta}^{(k)}|\mathbf{y})\}$  are the density values computed during a grid exploration on  $\tilde{\pi}(\boldsymbol{\theta}|\mathbf{y})$ . Since we do not have  $\tilde{\pi}(\boldsymbol{\theta}|\mathbf{y})$  evaluated at all points required to compute the integral in Eq. (4) we construct an interpolation  $I(\boldsymbol{\theta}|\mathbf{y})$  using the density values  $\{\tilde{\pi}(\boldsymbol{\theta}^{(k)}|\mathbf{y})\}$  computed during the grid exploration on  $\tilde{\pi}(\boldsymbol{\theta}|\mathbf{y})$  and approximate (4) by

$$\tilde{\pi}(\boldsymbol{\theta}_j|\mathbf{y}) = \int I(\boldsymbol{\theta}|\mathbf{y})d\boldsymbol{\theta}_{-j}. \quad (5)$$

Looking at [(3)-(5)] we can see that INLA can be divided into three main tasks, firstly propose an approximation  $\tilde{\pi}(\boldsymbol{\theta}|\mathbf{y})$  to the joint posterior of the hyperparameters  $\pi(\boldsymbol{\theta}|\mathbf{y})$ , secondly propose an approximation  $\tilde{\pi}(x_i|\boldsymbol{\theta}, \mathbf{y})$  to the marginals of the conditional distribution of the latent field given the data and the hyperparameters  $\pi(x_i|\boldsymbol{\theta}, \mathbf{y})$  and thirdly explore  $\tilde{\pi}(\boldsymbol{\theta}|\mathbf{y})$  on a grid and use it to integrate out  $\boldsymbol{\theta}$  in Eq. (3) and  $\boldsymbol{\theta}_{-j}$  in Eq. (5). A simplified algorithm would look like the following:

1. Select a set  $\Theta = \{\boldsymbol{\theta}^{(1)}, \dots, \boldsymbol{\theta}^{(K)}\}$
2. for  $k = 1, \dots, K$  do
3.     Compute  $\tilde{\pi}(\boldsymbol{\theta}^{(k)}|\mathbf{y})$
4.     Compute  $\tilde{\pi}(x_i|\boldsymbol{\theta}^{(k)}, \mathbf{y})$  as a function of  $x_i$  for all  $i$
5. end for
6. Compute  $\tilde{\pi}(x_i|\mathbf{y}) = \sum_k \tilde{\pi}(x_i|\boldsymbol{\theta}^{(k)}, \mathbf{y})\tilde{\pi}(\boldsymbol{\theta}^{(k)}|\mathbf{y}) \Delta\boldsymbol{\theta}^{(k)}$  as a function of  $x_i$ , for all  $i$ .

We refer to Rue et al. (2009) for details on how to perform the grid exploration to obtain  $\Theta = \{\boldsymbol{\theta}^{(1)}, \dots, \boldsymbol{\theta}^{(K)}\}$ , since it is not essential for understanding our proposed extension described in Section 3. Martins et al. (2013) discuss how to compute (5) efficiently.

The approximation used for the joint posterior of the hyperparameters  $\pi(\boldsymbol{\theta}|\mathbf{y})$  is

$$\tilde{\pi}(\boldsymbol{\theta}|\mathbf{y}) \propto \frac{\pi(\mathbf{x}, \boldsymbol{\theta}, \mathbf{y})}{\pi_G(\mathbf{x}|\boldsymbol{\theta}, \mathbf{y})} \Big|_{\mathbf{x}=\mathbf{x}^*(\boldsymbol{\theta})} \quad (6)$$

where  $\pi_G(\mathbf{x}|\boldsymbol{\theta}, \mathbf{y})$  is the Gaussian approximation (see Section 2.2) to the full conditional of  $\mathbf{x}$ , and  $\mathbf{x}^*(\boldsymbol{\theta})$  is the mode of the full conditional for  $\mathbf{x}$ , for a given  $\boldsymbol{\theta}$ . Expression (6) is equivalent to Tierney and Kadane (1986) Laplace approximation of a marginal posterior distribution, and it is exact if  $\pi(\mathbf{x}|\mathbf{y}, \boldsymbol{\theta})$  is a Gaussian.

For  $\pi(x_i|\boldsymbol{\theta}, \mathbf{y})$ , three options are available, and they vary in terms of speed and accuracy. The fastest option,  $\pi_G(x_i|\boldsymbol{\theta}, \mathbf{y})$ , is to use the marginals of the Gaussian approximation  $\pi_G(\mathbf{x}|\boldsymbol{\theta}, \mathbf{y})$  already computed when evaluating expression (6). The only extra cost to obtain  $\pi_G(x_i|\boldsymbol{\theta}, \mathbf{y})$  is to compute the marginal variances from the sparse precision matrix of  $\pi_G(\mathbf{x}|\boldsymbol{\theta}, \mathbf{y})$ . The Gaussian

approximation often gives reasonable results, but there can be errors in the location and/or errors due to the lack of skewness (Rue and Martino, 2007). The more accurate approach would be to do again a Laplace approximation, denoted by  $\pi_{LA}(x_i|\boldsymbol{\theta}, \mathbf{y})$ , with a form similar to expression (6)

$$\pi_{LA}(x_i|\boldsymbol{\theta}, \mathbf{y}) \propto \frac{\pi(\mathbf{x}, \boldsymbol{\theta}, \mathbf{y})}{\pi_{GG}(\mathbf{x}_{-i}|x_i, \boldsymbol{\theta}, \mathbf{y})} \Big|_{\mathbf{x}_{-i}=\mathbf{x}_{-i}^*(x_i, \boldsymbol{\theta})}, \quad (7)$$

where  $\pi_{GG}(\mathbf{x}_{-i}|x_i, \boldsymbol{\theta}, \mathbf{y})$  is the Gaussian approximation to  $\mathbf{x}_{-i}|x_i, \boldsymbol{\theta}, \mathbf{y}$  and  $\mathbf{x}_{-i}^*(x_i, \boldsymbol{\theta})$  is the modal configuration. A third option  $\pi_{SLA}(x_i|\boldsymbol{\theta}, \mathbf{y})$ , called simplified Laplace approximation, is obtained by doing a Taylor expansion on the numerator and denominator of expression (7) up to third order, thus correcting the Gaussian approximation for location and skewness with a much lower cost when compared to  $\pi_{LA}(x_i|\boldsymbol{\theta}, \mathbf{y})$ . We refer to Rue et al. (2009) for a detailed description of the Gaussian, Laplace and simplified Laplace approximations to  $\pi(x_i|\boldsymbol{\theta}, \mathbf{y})$ .

## 2.4 INLA and the importance of the Gaussian field

The main challenge in applying INLA to latent models is that the method depends heavily on the latent Gaussian prior assumption to work properly, both from the computational point of view and from the choice of approximations used as described in Section 2.3.

For the full conditional of  $\mathbf{x}$  to be well approximated by a Gaussian distribution in equations (6) and (7), we need it to be well behaved and close to a Gaussian. This is basically ensured by the latent Gaussian prior that is assigned to  $\mathbf{x}$  (see Stage 2 of Section 2.1) in latent Gaussian models, which has a non-negligible effect on the posterior, especially in terms of dependence between the components of  $\mathbf{x}$ .

Another important issue is that the conditional independence properties often encountered in the latent field translates into a sparse precision matrix when it is Gaussian distributed. This implies a huge decrease in computational time when performing the Gaussian approximation, which is extremely important since a Gaussian approximation needs to be computed for each value  $\boldsymbol{\theta}^{(k)}$  used on the grid for the numerical integration in Eq. (3).

## 3 Extension to near-Gaussian latent models

In this section we show how to extend the scope of INLA to include models similar in structure to the latent Gaussian models described in Section 2.1 but where the prior for some components of the latent field can have a near-Gaussian distribution. Section 3.1 will define these latent models in general while Section 3.2 will present an specific example, namely a survival model with gamma frailty. The proposed extension is then presented in Section 3.3.

### 3.1 Near-Gaussian latent models

The models we are interested in this paper has the same structure as the latent Gaussian models described in Section 2.1 with the exception that the latent field has some independent non-Gaussian components. We redefine stage 2 of the hierarchical model of Section 2.1 as

$$\text{Stage } \mathbf{2}^{new}. \underbrace{(\mathbf{x}_G, \mathbf{x}_{NG})}_{\mathbf{x}} | \boldsymbol{\theta}_2 \sim \pi(\mathbf{x} | \boldsymbol{\theta}_2) = \mathcal{N}(\mathbf{x}_G; \mathbf{0}, \mathbf{Q}^{-1}(\boldsymbol{\theta}_2)) \times \prod_i \pi(\mathbf{x}_{NGi} | \boldsymbol{\theta}_2),$$

where  $\mathbf{x}_G$  and  $\mathbf{x}_{NG}$  represent the Gaussian and non-Gaussian terms of the latent field, respectively. In addition we assume that  $\mathbf{x}_{NG}$  is formed by independent random variables. As a result, the distribution of the latent field is not Gaussian anymore, which precludes the use of INLA to fit this class of models.

The term *near-Gaussian* latent models refer to the restrictions we impose on the non-Gaussian components of the latent field. We aim for non-Gaussian distributions that are not too different from a Gaussian one, and are so that they could be well enough approximated by a Gaussian density. Although it is hard to give a precise definition of which distributions belong to the class of near-Gaussian distributions, we can restrict the possibilities by considering only distributions in which the density have full support on the real line, a unique and unimodal mode, finite first two moments and decreasing density as we move away from the mode. The main point here is to understand that our main interest in this paper lies on distributions that add flexibility around a Gaussian distribution, by correcting it in terms of skewness and/or kurtosis.

There are two main reasons for these restrictions. Firstly, it will imply that our proposed methodology returns accurate approximations for the posterior marginals of the non-Gaussian components, as will be shown in Section 3.3. Secondly, it fits the framework described in Section 1 in which we state that our ultimate goal is to include options in the R-INLA package so that the user could expand an initial model  $M_0$  based on Gaussian distributions in certain directions by adding flexibility around those Gaussian distributions, e.g. correcting it for asymmetry and/or kurtosis. This framework is an ongoing project and involves other considerations besides the computational methods presented here. For example, in this setting, we want the prior distributions for the hyperparameters to be chosen so that the extended model  $M_1$  could effectively be interpreted as an extension of the basic model  $M_0$ , i.e. in a way that  $M_0$  would have a central role within  $M_1$ . The INLA extension described in Section 3.3 is an essential component of this framework of more flexible models within R-INLA, and since the near-Gaussian distribution concept has a central role on this framework, it becomes important to understand that the concern here is with the design of algorithms that works well on this context of near-Gaussian latent



models.

There is no clear way to diagnose if a given non-Gaussian distribution fits the class of near-Gaussian distributions for the purpose of obtaining accurate results with our extension. Our experience have been that it works well for the cases we are currently interested in, which are distributions that correct the Gaussian in terms of skewness and/or kurtosis. However, the success of our extension has been verified on a case-by-case basis. This is not different than what have been done for most of the deterministic approximate methods for Bayesian inference. Our suggestion is to perform simulation studies to verify the accuracy of our approximations for each new class of non-Gaussian distribution that one might be interested.

### 3.2 Survival model - A first example

Consider the following exponential model that can be used to analyze survival data that comes from subjects of the same group who are related to each other or from multiple recurrence times of a event for the same individual. The likelihood

$$t_{ij} \sim \exp(\lambda_{ij}), \quad i = 1, \dots, I \text{ and } j = 1, \dots, J \quad (8)$$

is given by independent exponential distributions given  $\boldsymbol{\lambda} = \{\lambda_{ij}, i = 1, \dots, I, j = 1, \dots, J\}$ , where  $\lambda_{ij} = 1/\mu_{ij}$  and  $\mu_{ij}$  is the mean of  $t_{ij}$ . The index  $I$  could be interpreted as the number of groups in the data, while  $J$  would be the number of individuals in each group. This is a case of balanced data-set, but the unbalanced case could be treated just as easily by our method.

It is expected that individuals belonging to the same group are correlated with each other. This can be included in the model through the addition of random effects  $\boldsymbol{w} = \{w_1, \dots, w_I\}$  to account for variation between groups,

$$\eta_{ij} = \log(\lambda_{ij}) = \beta_0 + \beta_1 x_{ij} + \log w_i. \quad (9)$$

Besides the random effects, it is common to include some covariate effects that in our case are represented by the fixed effects  $\beta_0$  and  $\beta_1$ . In the survival analysis literature, the random effects are often called frailty and it is common to assume that they are Gamma distributed,  $w_i \sim \text{Gamma}(\kappa, \kappa)$ , with  $E(w_i) = 1$  to avoid identifiability issues. Notice that we have  $\log w_i$  in Eq. (9) only because this is how the model is defined in practice. That is,  $\lambda_{ij} = \exp\{\beta_0 + \beta_1\}w_i$ , hence Eq. (9). This is not to be confused with the application of log transformation to make the random effects' distribution closer to a Gaussian. Gaussian priors are assumed for the fixed effects and a Gamma prior is often used for the random-effect hyperparameter  $\kappa$ .

The latent field for this model is given by  $\mathbf{x} = (\boldsymbol{\eta}, \boldsymbol{\beta}, \mathbf{b})$ , with  $\mathbf{b} = \log(\mathbf{w})$  and it is non Gaussian since  $\mathbf{b}$  is formed by independent log-Gamma random variables,

$$\pi(\mathbf{b}|\kappa) = \prod_{i=1}^I \pi(b_i|\kappa) = \prod_{i=1}^I \frac{\kappa^\kappa}{\Gamma(\kappa)} \exp\{\kappa(b_i - \exp(b_i))\}. \quad (10)$$

Such a model cannot be applied straightforwardly using INLA since the assumption in Stage 2 is violated. However, it fits the class of models in Section 3.1 and will be further analyzed in Section 4.1 with our approach. Figure 1 shows a log-gamma distribution with  $\kappa = 1$  (solid line) and a Gaussian density (dashed line) with the same mean and precision as the log-gamma with  $\kappa = 1$ . We can see in Figure 1 that this log-gamma has negative skewness, positive kurtosis, and satisfy the desired properties of a near-Gaussian distribution as described in Section 3.1.

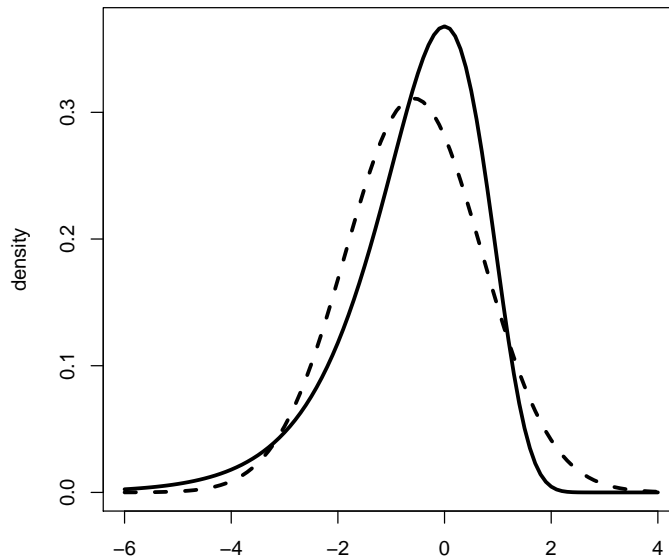


Figure 1: Log-gamma density (solid) with  $\kappa = 1$  and a Gaussian density (dashed) with the same mean and precision as the log-gamma density.

### 3.3 The extension

Given that INLA does not require the prior for  $\boldsymbol{\theta}$  to be Gaussian, a first approach to fit the class of models presented in Section 3.1 with INLA would be to include the non-Gaussian components

$\mathbf{x}_{NG}$  in the hyperparameters  $\boldsymbol{\theta}$  of the model. However, this is not a good idea in practice since the size of  $\mathbf{x}_{NG}$  is usually large and typically increase as the number of data points. This naive approach would lead to accurate results but the cost would be a large increase in computational time due to the grid exploration necessary to compute Eqs. (3)-(5). Basically, an increase in the dimension of  $\boldsymbol{\theta}$  would require a higher number of points  $\Theta = \{\boldsymbol{\theta}^{(1)}, \dots, \boldsymbol{\theta}^{(K)}\}$  to be evaluated during the grid exploration of  $\boldsymbol{\theta}$ . The approach presented next will deliver accurate results without the burden in computational time.

### 3.3.1 The main idea

Section 2.4 explained the importance of the latent Gaussian prior for INLA to run smoothly. With that in mind we propose to approximate the prior of the non-Gaussian components  $\pi(\mathbf{x}_{NG}|\boldsymbol{\theta}_2)$  by a Gaussian distribution  $\pi_G(\mathbf{x}_{NG}|\boldsymbol{\theta}_2)$  and correct this approximation by the correction term

$$CT = \pi(\mathbf{x}_{NG}|\boldsymbol{\theta}_2)/\pi_G(\mathbf{x}_{NG}|\boldsymbol{\theta}_2) \quad (11)$$

in the likelihood. This is, in fact, a way of writing a latent model of the form described in Section 3.1 into a latent Gaussian model, defined in Section 2.1.

The first stage is now formed by the original likelihood multiplied by the correction term

$$\prod_{i=1}^{n_d} \pi(y_i|x_i, \boldsymbol{\theta}_1) \times \pi(\mathbf{x}_{NG}|\boldsymbol{\theta}_2)/\pi_G(\mathbf{x}_{NG}|\boldsymbol{\theta}_2).$$

Another way of writing this is to define an extended response vector  $\mathbf{z}$ , with  $z_i = y_i$  if  $i \leq n_d$  and  $z_i = 0$  if  $n_d < i \leq n_d + k$ , where  $k$  is the length of  $\mathbf{x}_{NG}$  and write

**Stage 1.**  $\mathbf{z}|\mathbf{x}, \boldsymbol{\theta} \sim \pi(\mathbf{z}|\mathbf{x}, \boldsymbol{\theta}) = \prod_{i=1}^{n_d+k} \pi(z_i|x_i, \boldsymbol{\theta})$ , where

$$\pi(z_i|x_i, \boldsymbol{\theta}) = \begin{cases} \pi(y_i|x_i, \boldsymbol{\theta}_1) & \text{for } 1 \leq i \leq n_d \\ \pi(x_{NG,i}|\boldsymbol{\theta}_2)/\pi_G(x_{NG,i}|\boldsymbol{\theta}_2) & \text{for } n_d < i \leq n_d + k \end{cases} \quad (12)$$

It is important to emphasize that Stage 1 above is not the likelihood function, but expressing the model using this form will make the description and implementation of the algorithm that follows easier. The latent field has now a Gaussian approximation replacing the non-Gaussian distribution of  $\mathbf{x}_{NG}$ ,

**Stage 2.**  $\underbrace{(\mathbf{x}_G, \mathbf{x}_{NG})}_{\mathbf{x}}|\boldsymbol{\theta}_2 \sim \pi(\mathbf{x}|\boldsymbol{\theta}_2) = \mathcal{N}(\mathbf{x}_G; \boldsymbol{\mu}(\boldsymbol{\theta}_2), \mathbf{Q}^{-1}(\boldsymbol{\theta}_2)) \times \pi_G(\mathbf{x}_{NG}|\boldsymbol{\theta}_2)$ ,

which means that now  $\pi(\mathbf{x}|\boldsymbol{\theta}_2)$  is Gaussian distributed. The third stage is once again formed by the prior distribution on the hyperparameters,

**Stage 3.**  $\boldsymbol{\theta} \sim \pi(\boldsymbol{\theta})$ .

Independent of the Gaussian approximation  $\pi_G(\mathbf{x}_{NG}|\boldsymbol{\theta}_2)$  used, the hierarchical model above is equivalent to the model described in Section 3.1. Considerations on how to choose this Gaussian approximation and how this model formulation will help us to perform inference will be presented soon, but first we can rewrite the survival model of Section 3.2 in this new formulation.

### Survival model (Cont.)

For the survival model defined in Section 3.2, we have that the original likelihood function, defined in Eq. (8), is an exponential distribution

$$\log \pi(t_{ij}|\eta_{ij}) = \eta_{ij} - \exp(\eta_{ij}t_{ij}),$$

where  $\eta_{ij}$  is the linear predictor defined in Eq. (9). Based on Eq. (10) the correction term (see Eq. (11)) is given by

$$\begin{aligned} CT &= \prod_{i=n_d+1}^{n_d+I} \pi(\mathbf{x}_{NG,i}|\boldsymbol{\theta}_2)/\pi_G(\mathbf{x}_{NG,i}|\boldsymbol{\theta}_2) \\ &= \prod_{i=1}^I \pi(b_i|\kappa)/\pi_G(b_i|\mu_b, \tau_b) = \prod_{i=1}^I CT_i, \end{aligned}$$

with

$$\log CT_i = \kappa(b_i - \exp(b_i)) + \frac{\tau_b(\kappa)}{2}(b_i - \mu_b(\kappa))^2 + \text{const}, \quad (13)$$

where  $\mu_b(\kappa)$  and  $\tau_b(\kappa)$  are the mean and precision parameter of the Gaussian approximation to the log-Gamma random effects  $\mathbf{b}$  and const is a constant that does not depend on  $\mathbf{b}$ . The latent field  $\mathbf{x} = (\boldsymbol{\eta}, \mathbf{b}, \boldsymbol{\beta})$  is now Gaussian since  $\pi(\mathbf{b}|\kappa)$  is approximated by  $\pi_G(\mathbf{b}|\mu_b(\kappa), \tau_b(\kappa)) = \mathcal{N}(\mathbf{b}; \mu_b(\kappa)\mathbf{1}_I, \tau_b(\kappa)^{-1}\mathbf{I}_I)$ , where  $\mathbf{1}_n$  is a vector of ones with dimension  $n$  and  $\mathbf{I}_n$  is an  $n \times n$  identity matrix.

### 3.3.2 Computational considerations

At first sight, it seems obvious that once our latent (non-Gaussian) model of interest has been rewritten into a latent Gaussian model we could apply INLA to obtain the posterior marginals of interest. However, we need to understand what are the consequences of this change within the INLA framework. The main change is on the Gaussian approximation to the full conditional of the latent field (see Section 2.2), that now takes the form

$$\pi(\mathbf{x}|\boldsymbol{\theta}, \mathbf{y}) \propto \exp \left\{ -\frac{1}{2}\mathbf{x}^T \mathbf{Q}(\boldsymbol{\theta})\mathbf{x} + \sum_{i=1}^{n_d} g_i(x_i) + \sum_{i=n_d+1}^{n_d+k} h_i(x_i) \right\}, \quad (14)$$

where  $g_i(x_i) = \log \pi(y_i|x_i, \boldsymbol{\theta})$  as before and

$$h_i(x_i) = \log CT_i = \log \pi(\mathbf{x}_{NG,i}|\boldsymbol{\theta}_2) - \log \pi_G(\mathbf{x}_{NG,i}|\boldsymbol{\theta}_2).$$

It was shown in Section 2.2 that a Gaussian approximation is obtained by approximating the non-quadratic functions, in this case  $g_i(x_i)$  and  $h_i(x_i)$ , by quadratic functions using Taylor expansion up to second order. Once we know we are dealing with a well behaved log likelihood function  $g_i(x_i)$  as, for example, those belonging to the exponential family, the success of a Gaussian approximation to Eq. (14) will depend heavily on the shape of  $h_i(x_i)$ .

For instance, it is desirable to have a bounded correction term

$$\pi_{NG}(\cdot|\boldsymbol{\theta})/\pi_G(\cdot|\boldsymbol{\theta}) < \infty$$

for a quadratic form approximation to  $h_i(x_i)$  to make sense. This implies that the Gaussian approximation  $\pi_G(\mathbf{x}_{NG}|\boldsymbol{\theta})$  should ideally dominate  $\pi_{NG}(\mathbf{x}_{NG}|\boldsymbol{\theta})$  in the sense that it should have thicker tails than the non-Gaussian distribution it is trying to approximate. But in practice, it is sufficient to have a bounded correction term on the region that concentrates the bulk of probability mass since we can afford a bigger approximation error on the region that doesn't contribute much to the density (14). In our examples, we have chosen  $\pi_G(\cdot|\boldsymbol{\theta})$  to be a Gaussian distribution with zero mean ( $\mu = 0$ ) and low precision ( $\tau \rightarrow 0$ ) to approximate the distribution of the non-Gaussian components  $\pi_{NG}(\cdot|\boldsymbol{\theta})$ . This choice satisfy the bounded correction term requirement and since it does not depend on  $\boldsymbol{\theta}$ , it avoids the complication of computing a new Gaussian approximation for each value of  $\boldsymbol{\theta}$  in the grid exploration.

Although not necessary, it is desirable to have both the correction term  $\exp\{h_i(x_i)\}$  and the likelihood function  $\exp\{g_i(x_i)\}$  to be log-concave, at least on a neighborhood of the mode of Eq. (14). This would imply  $\pi(\mathbf{x}|\boldsymbol{\theta}, \mathbf{y})$  defined in Eq. (14) to be log-concave. It is easier to design an algorithm to maximize a concave function. For example, a quadratic model function provides a good local approximation to the objective function being maximized. This can be seen in Section 2.2 where we propose to maximize Eq. (2) by performing a series of quadratic approximations. The mode  $\boldsymbol{\mu}^*$  is then found iteratively by solving the linear system

$$\mathbf{Q}'(\boldsymbol{\mu}^{(j-1)})\boldsymbol{\mu}^{(j)} = \mathbf{b}(\boldsymbol{\mu}^{(j-1)}) \tag{15}$$

until convergence is attained, where  $\mathbf{Q}'(\boldsymbol{\mu}^{(j-1)}) = \{\mathbf{Q} + \text{diag}(\mathbf{c}(\boldsymbol{\mu}^{(j-1)}))\}$  and  $\mathbf{Q}$ ,  $\mathbf{b}$  and  $\mathbf{c}$  are defined in Section 2.2. This is equivalent to a Newton-Raphson algorithm.

Next, we show that the survival model in Section 3.2 is one example where both the correction term and the likelihood function are log-concave.

### Survival model (Cont.)

For the survival model, we have a log-concave likelihood function as we can see in Figure 2, where we have the plots of the log likelihood and the second derivative of the log likelihood for a given data point, assuming different values for the data point.

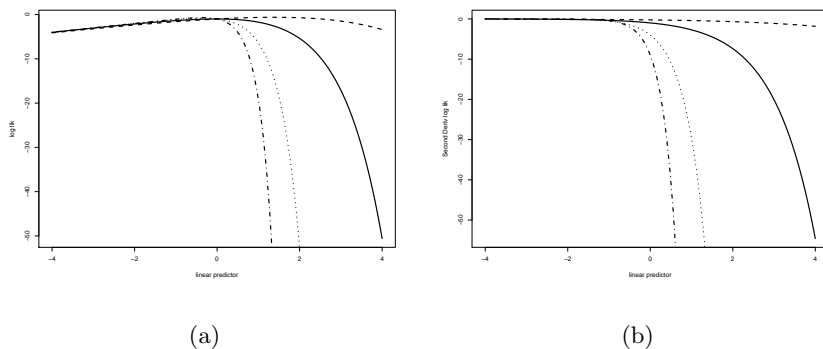


Figure 2: Plot of the log likelihood (a) and of the second derivative of the log likelihood (b) against the linear predictor for different values of data points for the survival model. It was used the following values for the data point: 0.5 (Dashed), 1 (Solid), 2 (Dotted) and 3 (Dot-dash)

If we use a zero mean and low precision Gaussian distribution ( $\mu_b = 0$  and  $\tau_b \rightarrow 0$ ) in Eq. (13) we also attain a log-concave correction term,

$$\log CT_i = \kappa(b_i - \exp(b_i)) + \text{const} \quad (16)$$

as illustrated in Figure 3.

□

The example in Section 4.2 considers a linear mixed-effects model where both the likelihood and the random effects are distributed according to a Student's t distribution. This is a case where both the likelihood and the correction term are not log-concave. This brings an extra challenge for the optimization of  $\pi(\mathbf{x}|\boldsymbol{\theta}, \mathbf{y})$  in Eq. (14). We have obtained good results using trust region methods (Conn et al., 1987), which are well known in the optimization literature. In our context, we constrain or expand the subset of the domain, known as trust region, where a quadratic function is used to approximate the objective function  $\pi(\mathbf{x}|\boldsymbol{\theta}, \mathbf{y})$  to be optimized.

We accomplish this by iteratively solving

$$\{\mathbf{Q}'(\boldsymbol{\mu}^{(j-1)}) + \delta \text{diag}(\mathbf{Q}'(\boldsymbol{\mu}^{(j-1)}))\} \boldsymbol{\mu}^{(j)} = \mathbf{b}(\boldsymbol{\mu}^{(j-1)})$$

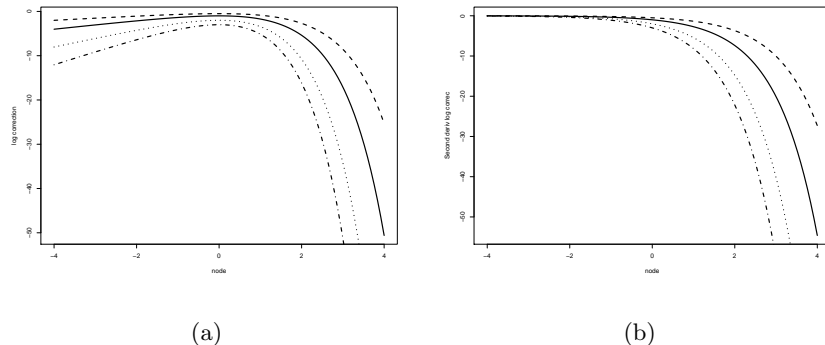


Figure 3: Plot of the log correction term (a) and of the second derivative of the log correction term (b) against  $b_i$  for different values of  $\kappa$  for the survival model. It was used the following values for  $\kappa$ : 0.5 (Dashed), 1 (Solid), 2 (Dotted) and 3 (Dot-dash)

instead of Eq. (15), where  $\delta$  is the parameter that control the trust-region size. At each iteration we expand the trust region by decreasing  $\delta$  if the quadratic approximation to  $\pi(\mathbf{x}|\boldsymbol{\theta}, \mathbf{y})$  is adequate. On the other hand, we shrink the trust region by increasing  $\delta$  if the quadratic approximation is not adequate. When we get close to the mode  $\boldsymbol{\mu}^*$ , the quadratic function becomes a good approximation to  $\pi(\mathbf{x}|\boldsymbol{\theta}, \mathbf{y})$ , in which case we can set  $\delta$  to zero and return to the original optimization problem given by Eq. (15).

Trust-region methods have a nice Bayesian interpretation in this context. The use of  $\delta > 0$  in this case could be interpreted as an increase in the precision of the prior of the latent field. This solution is in agreement with the findings of Vanhatalo et al. (2009). They have found, in the context of a Student’s t likelihood, that the most problematic case in the optimization of a non log-concave full conditional of the type (14) happens when the prior is much wider than the likelihood, in which case moderate prior-data conflict can lead to numerical instability. By increasing the precision of the prior in the moments of numerical instability, we allow the algorithm to proceed until a point close to the mode, where  $\delta$  is set to zero and the original prior is recovered.

### 3.3.3 Checking accuracy

We can use the same tools described in Rue et al. (2009) to assess the approximation error of our approach. The accuracy of  $\tilde{\pi}(\boldsymbol{\theta}|\mathbf{y})$  is directly related to the “effective” dimension of the latent field  $\mathbf{x}$ . The package **R-INLA** returns the expected number of effective parameters,  $E_{\text{eff}}$ . In general, if  $E_{\text{eff}} < n_d/2$  we have strong evidence that the Gaussian approximation to  $\pi(\mathbf{x}|\boldsymbol{\theta}, \mathbf{y})$

in Eq. (14) is adequate, where  $n_d$  is the number of data points.

The second strategy is based on the idea of comparing elements of a sequence of increasingly accurate approximations. By default, **R-INLA** computes the symmetric Kullback-Leibler divergence (SKLD) between the integrated marginals in Eq. (3) obtained using the Gaussian and the simplified Laplace approximation to  $\pi(x_i|\boldsymbol{\theta}, \mathbf{y})$ , respectively. If the divergence is small then both approximations are considered as acceptable. Otherwise, one should compute Eq. (3) using the Laplace approximation to  $\pi(x_i|\boldsymbol{\theta}, \mathbf{y})$  and check the SKLD between this and the one obtained with the simplified Laplace approximation. Again, if the divergence is small, simplified Laplace and Laplace approximations appear to be acceptable; otherwise, the Laplace approximation is our best estimate, but further investigation might be required to check the quality of the approximations.

Needless to say, those strategies are not fail proof. The only way to assess with certainty the approximation of our approach would be to run a MCMC sampler for an infinite time; and even if this was possible, we would need a way to check with certainty if the MCMC chain have converged to the correct stationary distribution, which is also not an easy task.

## 4 Examples

We now proceed to two examples where we apply the methodology proposed in this paper and compare the results with that obtained by MCMC. Comparison with MCMC has no practical value and is presented here only to convince the reader that with only a small fraction of computational time our approach gives similar accuracy when compared with MCMC algorithms. In practice, we suggest to use the tools presented in Section 3.3.3 to check the accuracy of the approximations. The INLA software is in constant development, but support regarding the code used in this paper can be found at the INLA website (<http://www.r-inla.org/>).

### 4.1 Survival analysis with Gamma frailty

Here we apply our proposed extension to fit the model defined in Section 3.2 in a simulated data-set and compare the results with that obtained by MCMC. For the experiment reported we have simulated 100 groups, each of which with 10 individuals. The covariates  $\{x_{ij}\}$  in Eq. (9) were simulated from a uniform distribution on the interval  $(0, 1)$  while the frailties came from a Gamma distribution with both the shape and rate parameters equal to 1. The fixed effects  $\beta_0$  and  $\beta_1$  were chosen to be 1.

We use OpenBUGS (Lunn et al., 2009) to generate samples from the posterior distribution.



Figure 4(a) shows the posterior mean of the log frailties  $\{b_i : b_i = \log w_i, i = 1, \dots, 100\}$  obtained by INLA (x-axis) and by MCMC (y-axis). An identity function is also plotted in order to help visualize the strong agreement between both methods. Figure 4(b) display the histogram formed by the samples of  $\pi(b_{80}|\mathbf{y})$  returned by OpenBUGS and the line is the approximated posterior computed using our extension. This specific component was chosen at random, since similar accuracy was obtained for all log frailties in our simulation study. Figure 5 show similar pictures for  $\beta_1$  and  $\kappa$  to show that the excellent results are also valid for the fixed effects and for the hyperparameter  $\kappa$  of our model. The R code used to run INLA in this example is available in Appendix A.

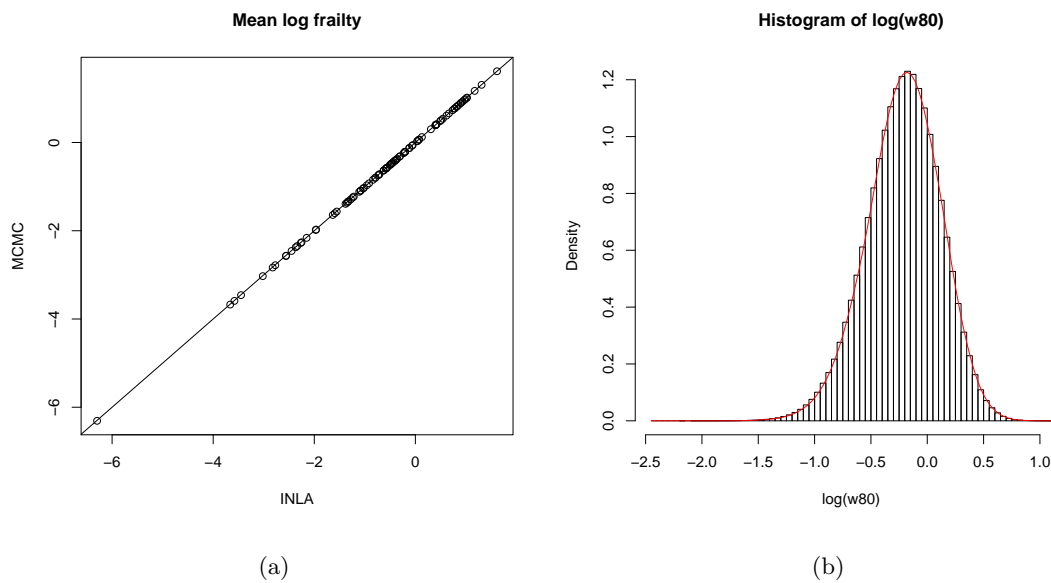


Figure 4: Comparison between INLA and MCMC for the exponential gamma frailty example: (a) Plot of the posterior mean of the log frailties returned by INLA (x-axis) vs. MCMC (y-axis). (b) Approximate posterior density for  $\log w_{80}$  obtained by INLA (solid line) and by MCMC (histogram).

It is important to note that the comparisons with MCMC were made with millions of samples, taking minutes to run, since for short to medium number of samples it was possible to visually detect errors in the MCMC estimates when compared to INLA, that took a little bit more than 1 second to run on a Intel Core i5 with 2.67GHz. One can argue that the number of samples (and time) necessary by a MCMC scheme to attain the desired accuracy of our application could be reduced if more time was spent designing a specific MCMC scheme for this particular application instead of using the general purpose OpenBUGS. Although this is true in theory, we

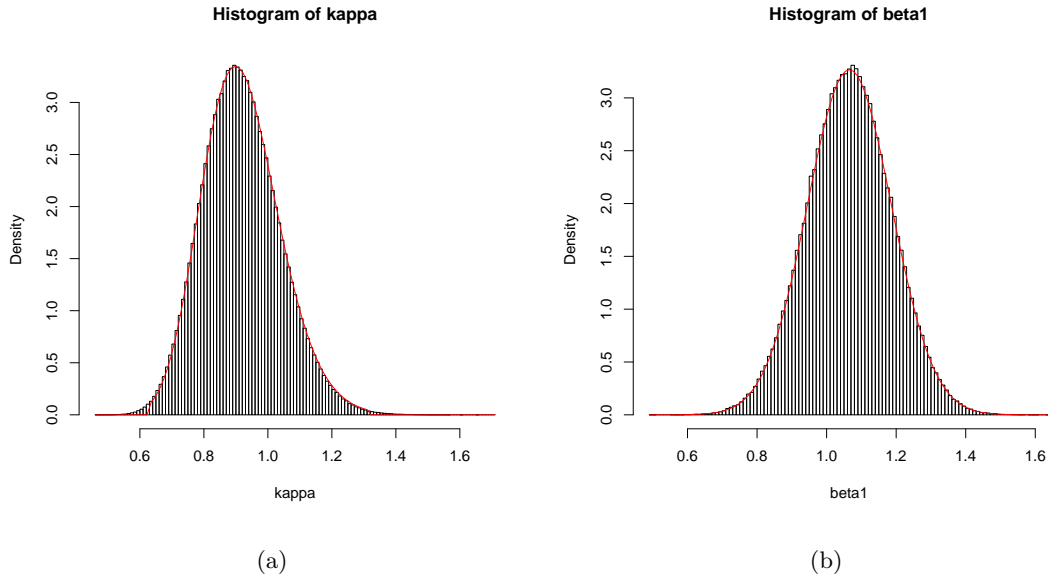


Figure 5: Comparison between INLA and MCMC for the exponential gamma frailty example: (a) Approximate posterior density for  $\kappa$  obtained by INLA (solid line) and by MCMC (histogram) (b) Approximate posterior density for  $\beta_1$  obtained by INLA (solid line) and by MCMC (histogram)

are here comparing two general purpose tools for the class of latent models into consideration, and even with a tailored MCMC scheme, we believe that the difference in time will still be in orders of magnitude, not to mention the time necessary to develop specific algorithms for each new model belonging to this same class.

## 4.2 Robust mixed-effects models using Student-t distribution

In this example, we show our method applied to a Bayesian random effects model where the random effects have an Student-t distribution. Assume we have data  $\{\mathbf{y}_i; i = 1, \dots, n\}$  recorded for  $n$  groups each having  $k_i$  individuals. Assume that  $\mathbf{y}_i$ 's are independent Gaussian random vector described by the following standard mixed effect model (Laird and Ware, 1982), useful to analyze repeated measures or grouped data,

$$\mathbf{y}_i = \mathbf{X}_i \boldsymbol{\beta} + b_i + \mathbf{e}_i, \quad (17)$$

where both the random effect  $b_i$  and the error term  $\mathbf{e}_i$  have a Gaussian distribution,  $b_i \sim N(0, \sigma_b^2)$  and  $\mathbf{e}_i \sim N(0, \sigma_e^2 \mathbf{I})$  with variances  $\sigma_b^2$  and  $\sigma_e^2$  respectively, being  $\mathbf{I}$  a  $(k_i \times k_i)$  identity matrix.  $\mathbf{X}_i$  represent the  $(k_i \times p)$  design matrix for group  $i$  and  $\boldsymbol{\beta}$  is a  $(p \times 1)$  vector of fixed effects.

Statistical inference based on the Gaussian distribution is known to be vulnerable to outliers. One approach to more robust modeling is to replace the Gaussian distribution by Student-t distribution in the model. In the context of linear mixed effects model, Pinheiro et al. (2001) suggested to follow the robust statistical modeling approach described by Lange et al. (1989) in which the Gaussian distributions of  $b_i$  and  $e_i$  are replaced by  $t$ -distributions,

$$b_i \sim t(0, \psi_b^2, \nu), \quad e_i \sim t(0, \psi_e^2 \mathbf{I}, \nu), \quad (18)$$

where  $\psi_b^2$  and  $\psi_e^2$  are the scale parameters and  $\nu$  is the common degree of freedom parameter. They also noted that in mixed effects models the outlier may occur either at the level of within-group error  $e_i$ , called  $e$ -outliers, or at the level of random effects  $b_i$ , called  $b$ -outliers. This approach can be regarded as outlier accommodation although it provides useful information for outlier identification. For the simulation experiment performed later in this Section, we have used a Gamma prior with shape and rate parameters given by 1 and 0.1 respectively for the inverse scale parameters, a Gaussian distribution with mean zero and low precision ( $10^{-4}$ ) for the fixed effects and a Gaussian distribution with mean 3 and variance 1 for  $\nu^* = \log(\nu - 5)$ , so that the bulk of prior probability mass is between 7 and 150 for the degree of freedom parameter  $\nu$ . Note that we have defined  $\nu^*$  so that  $\nu > 5$  in order to get a well defined first four moments of the Student-t distribution.

The model (17)-(18) has the likelihood function formed by a  $t$  distribution

$$y_{ij} | \mathbf{x}, \boldsymbol{\theta} \sim t(\eta_{ij}, \psi_e^2, \nu), \quad i = 1, \dots, n \text{ and } j = 1, \dots, k_i,$$

which does not belong to the exponential family, where  $\eta_{ij}$  is the linear predictor

$$\eta_{ij} = \mathbf{X}_i \boldsymbol{\beta} + b_i.$$

The latent field is then formed by  $\mathbf{x} = (\boldsymbol{\eta}, \mathbf{b}, \boldsymbol{\beta})$ , where  $\mathbf{b} = \{b_i; i = 1, \dots, n\}$  is formed by independent  $t$  distributed random variables and has therefore a non-Gaussian distribution given by

$$\pi(\mathbf{b} | \psi_b^2, \nu) = \prod_{i=1}^n \pi(b_i | \psi_b^2, \nu) = \prod_{i=1}^n \frac{\Gamma(\frac{\nu+1}{2})}{\Gamma(\frac{\nu}{2})} (\psi_b^2 \pi \nu)^{-1/2} \left[ 1 + \frac{b_i^2}{\psi_b^2 \nu} \right]^{-(\nu+1)/2} \quad (19)$$

If we use Eq. (11) and (19) we get the following log correction term

$$\begin{aligned} \log CT_i &= \log \pi(b_i | \psi_b^2, \nu) - \log \pi_G(b_i | \mu_b, \tau_b) \\ &= -\frac{(\nu+1)}{2} \log \left\{ 1 + \frac{b_i^2}{\psi_b^2 \nu} \right\} + \frac{\tau_b}{2} (b_i - \mu_b)^2 + \text{const.} \end{aligned}$$

Again, if we assume a zero mean and low precision Gaussian distribution ( $\mu_b = 0$  and  $\tau_b \rightarrow 0$ ) we end up with

$$\log CT_i = -\frac{(\nu + 1)}{2} \log \left\{ 1 + \frac{b_i^2}{\psi_b^2 \nu} \right\} + \text{const.}$$

Figure 6 show plots of the second derivative of the likelihood (Figure 6(a)) and of the log correction (Figure 6(b)) term assuming a data point  $y = 1$ , variances  $\psi_e^2 = 1$ ,  $\psi_b^2 = 1$  and different values for  $\nu$  ( $\nu = 5, 10, 20, 50$ ).

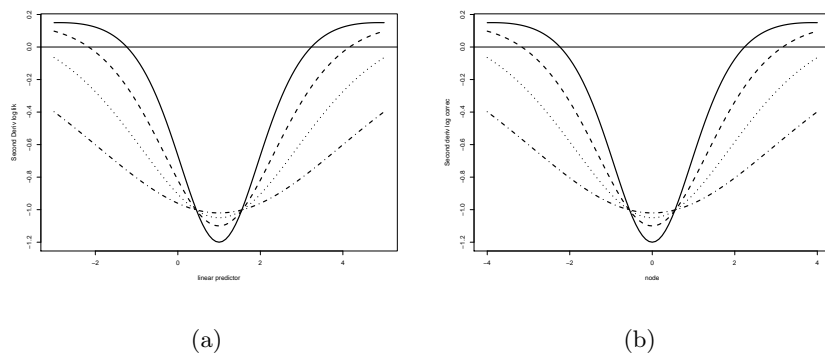


Figure 6: (a) Plot of the second derivative of the log likelihood against linear predictor for  $\psi_e^2 = 1$ ,  $y = 1$  and different values of  $\nu$  and (b) plot of the second derivative of the log correction term against  $b_i$  for  $\psi_b^2 = 1$  and different values of  $\nu$  for the t-mixed effect model. It was used the following values for  $\nu$ : 5 (Solid), 10 (Dashed), 20 (Dotted) and 50 (Dot-dash).

We have here an example where both the likelihood and the correction term are not log-concave, specially for low values of degree of freedom parameter  $\nu$ . As explained in Section 3.3.2, our extension can be applied to models where the likelihood and/or correction term are not log-concave. We use trust region methods to make the optimization of  $\tilde{\pi}(\mathbf{x}|\boldsymbol{\theta}, \mathbf{y})$  more robust.

Now we can proceed to a contamination study similar to that performed in Pinheiro et al. (2001). Here we have data simulated from

$$y_i = X\beta + b_i + e_i, \quad i = 1, \dots, 27, \quad X = \begin{bmatrix} 1 & 8 \\ 1 & 10 \\ 1 & 12 \\ 1 & 14 \end{bmatrix} \quad (20)$$

with the following mixture of Gaussian models being used to contaminate the distributions of

the  $b_i$  and the  $e_i$ .

$$\begin{aligned} b_i &\stackrel{ind}{\sim} (1 - p_b)\mathcal{N}(0, \sigma_b^2) + p_b f \mathcal{N}(0, \sigma_b^2) \\ e_i &\stackrel{ind}{\sim} (1 - p_e)\mathcal{N}(0, \sigma_e^2) + p_e f \mathcal{N}(0, \sigma_e^2), \quad i = 1, \dots, 27, \quad j = 1, \dots, 4 \end{aligned}$$

where  $p_b$  and  $p_e$  denote, respectively, the expected percentage of  $\mathbf{b}$ - and  $\mathbf{e}$ -outliers in the data and  $f$  denotes the contamination factor. The true parameters for the uncontaminated distributions are  $\sigma_b^2 = 3$  and  $\sigma_e^2 = 2$ , while the true values for the fixed effects are  $\beta = (12, 1)^T$ .

All 32 combinations of  $p_b, p_e = 0, .05, .1, .25$ , and  $f = 2, 4$  were used in the simulation study. The  $f = 2$  case corresponds to a close contamination pattern, while  $f = 4$  illustrates a more distant contamination pattern. A total of 500 Monte Carlo replications were obtained for each  $(p_b, p_e, f)$  combination.

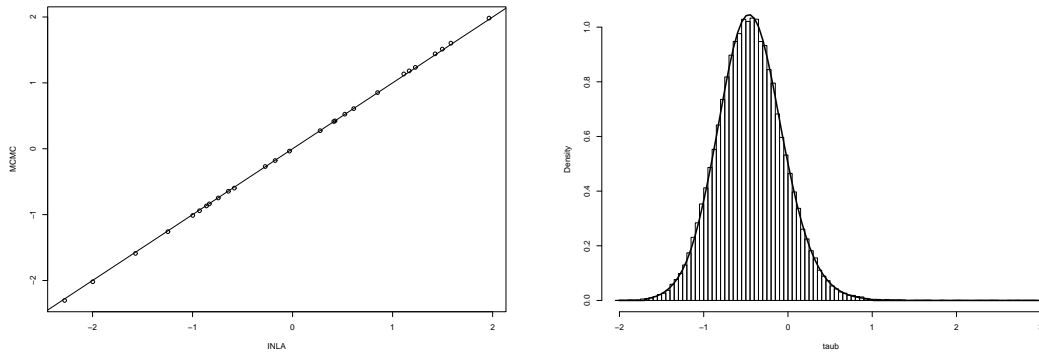
Let  $\theta$  denote a parameter of interest, with target value  $\theta_0 \neq 0$ , estimated by  $\hat{\theta}$ , which in our case will be the posterior mean of  $\theta$ . The efficiency of the Gaussian estimator  $\hat{\theta}_G$  relative to the multivariate  $t$  estimator  $\hat{\theta}_T$  is defined as the ratio of the respective mean square errors,

$$E(\hat{\theta}_G - \theta_0)^2 / E(\hat{\theta}_T - \theta_0)^2, \quad (21)$$

where expectations are taken with respect to the simulation distribution, that is  $E(\widehat{\hat{\theta}} - \theta_0)^2 = \sum_{i=1}^{500} (\hat{\theta}_i - \theta_0)^2 / 500$ .

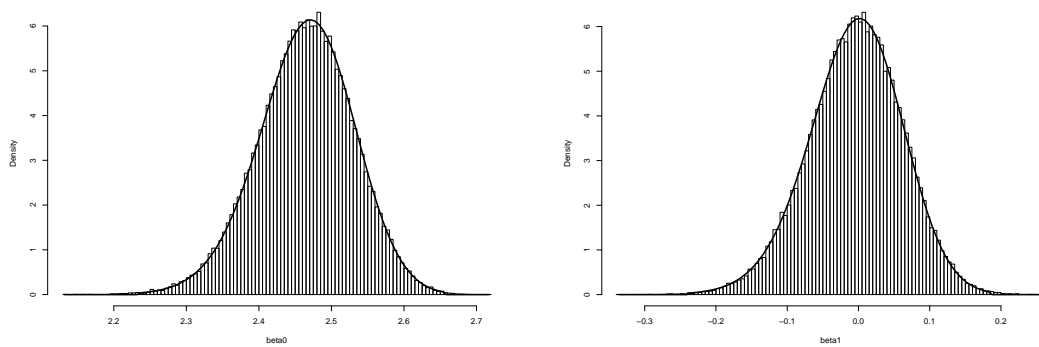
We have chosen some data-sets out of the  $32 \times 500 = 16000$  used in this contamination study and fitted the model using both MCMC and INLA to make sure that INLA is doing at least as good as MCMC in terms of accuracy. After that we proceed with the contamination study with INLA as the only estimation method as it would be impractical to fit all 16000 data-sets with MCMC. Figures 7 and 8 illustrate this comparison for one of the data-sets, where Figure 7(a) display the log random effects returned by INLA (x-axis) vs. MCMC (y-axis), while Figures 7(b) and 8 display the approximate posterior densities for  $\log \tau_b = \log 1/\psi_b^2$  and for the log fixed effects  $\log \beta_0$  and  $\log \beta_1$  respectively, obtained by INLA (solid line) and by MCMC (histogram).

Figures 9 and 10 plots the relative efficiency, defined in Eq. (21), between the posterior means of the  $t$  model over the Gaussian linear mixed effects model. Based on the plots the conclusion of our simulation study are, as expected, similar to that obtained by Pinheiro et al. (2001). There are substantial gains in efficiency for all parameters under the more distant contamination pattern ( $f = 4$ ) and moderate gains under the close contamination pattern ( $f = 2$ ). The efficiency gains are bigger for the precision of the random effects and the non-monotonic behavior of the efficiency gains suggest that the  $t$  model is more robust than the Gaussian model especially for moderate percentage (5 – 10%) of outliers. The two methods have about the same efficiency under the no-contamination case.



(a) Plot of the posterior mean of the log random effects returned by INLA (x-axis) vs. MCMC (y-axis). (b) Approximate posterior density for  $\log \tau_b = \log 1/\psi_b^2$  obtained by INLA (solid line) and by MCMC (histogram)

Figure 7: Comparison between INLA and MCMC for the robust mixed effect model.

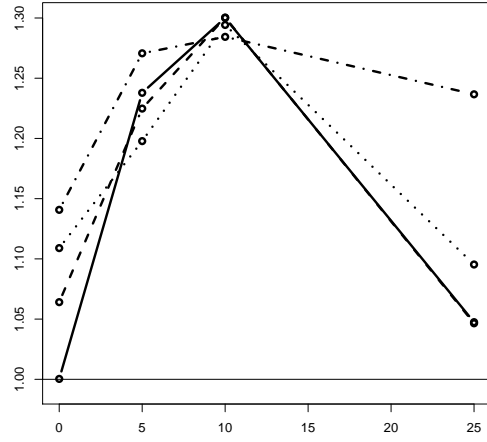
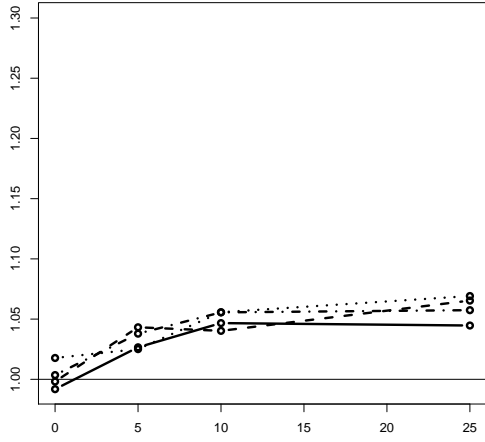


(a) Approximate posterior density for  $\log \beta_0$  obtained by INLA (solid line) and by MCMC (histogram) (b) Approximate posterior density for  $\log \beta_1$  obtained by INLA (solid line) and by MCMC (histogram)

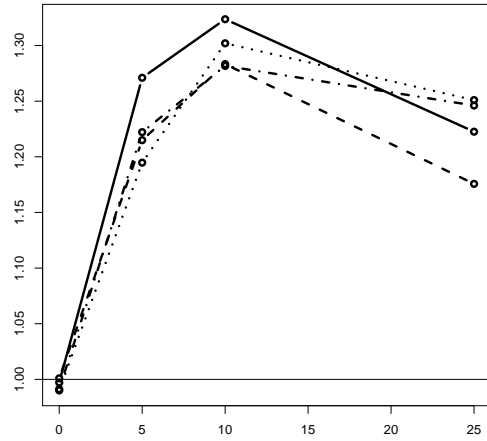
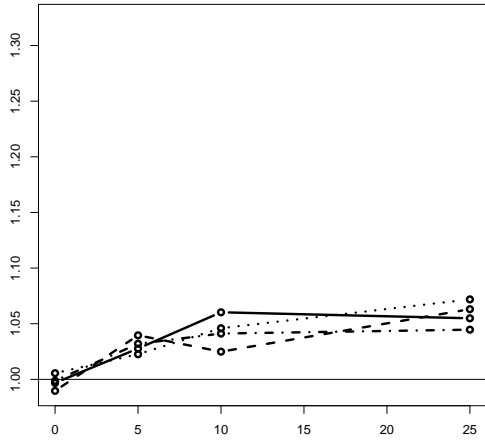
Figure 8: Comparison between INLA and MCMC for the robust mixed effect model.

## 5 Conclusion

INLA is a deterministic approach to perform approximate fully Bayesian inference on the class of LGMs. It is not meant to be a replacement of MCMC in general, but it is shown to work extremely well in the broad class of LGMs, where it delivers accurate results with only a small fraction of computational time, when compared to MCMC. Although many standard models



(a)  $\beta_0$  under close contamination pattern ( $f = 2$ ) (b)  $\beta_0$  under distant contamination pattern ( $f = 4$ )



(c)  $\beta_1$  under close contamination pattern ( $f = 2$ ) (d)  $\beta_1$  under distant contamination pattern ( $f = 4$ )

Figure 9: Relative efficiency (see Eq. (21)) of the  $t$  posterior mean with respect to the Gaussian posterior mean for the fixed effects in the linear mixed effect example. It plots the efficiency on the y-axis and  $p_e$  on the x-axis. The meaning for the different types of lines are: (Solid line)  $p_b = 0\%$ , (Dashed line)  $p_b = 5\%$ , (Dotted line)  $p_b = 10\%$  and (Dot-sash line)  $p_b = 25\%$ .

currently in use by the applied community fall within the class of LGMs, it is often necessary to build more flexible models that go beyond the Gaussian distribution for some of the latent com-

ponents. This paper describes the INLA extension that allow us to fit these more flexible models within the INLA framework. The main idea is to approximate the non-Gaussian components of the latent field with a Gaussian distribution and correct this approximation with a correction term in the likelihood. This solution preserves the Gaussian nature of the latent field, which is of extreme importance for the INLA method. At the same time, it preserves the non-Gaussianity of the latent field in the model formulation. We have discussed the impact of this new formulation within the INLA methodology. Also, computational considerations regarding the use of INLA in this more complex models were described. Our approach works well for distributions that add flexibility around the Gaussian by correcting it in terms of skewness and/or kurtosis, which we denote as near-Gaussian distributions.

Two examples of interest were given. The first, survival model with gamma frailty, has log-concave likelihood and correction term, and is therefore considered easier from an optimization point of view. The second, a linear mixed model with Student's  $t$  distribution for the error term and for the random effects, is more challenging since both the likelihood and the correction term are not log-concave. Our approach has provided very accurate approximations for posterior marginals and summaries for both examples when compared with very long MCMC runs. The comparison with MCMC is made only for illustrative purposes, since the whole point of our approach is to avoid the use of time consuming MCMC algorithms. One nice property of our approach is that the same techniques described in Rue et al. (2009) to check the accuracy of the the approximations can still be used. A summary of these techniques were presented.

Our extension can be used to fit non-Gaussian state space models (Kitagawa, 1987) where the distribution of the noise in the state space evolution equation is assumed to be non-Gaussian and will be discussed elsewhere. There is also a plan to extend the R package INLA to include options that allow the user to add flexibility and challenge the Gaussian assumptions of some components of the latent field in a straightforward and intuitive way. The focus of this extension will be on near-Gaussian distributions, and the method presented here will be used as the inference tool.

## A R code - Survival model

Following is the INLA code used in example 4.1. The code below show how we apply our idea of approximating the non-Gaussian components of the latent field by a Gaussian distribution and correcting this approximation with a correction term in the likelihood. The faked observations is what allow us to include the correction term in the likelihood. Notice that the `family` argument in the `inla` function is what determine what is the "likelihood" of this faked observations, which



in this case is the correction term in Eq. (13), defined as "loggammafrailty" in R-INLA. The expression

```
f(loggamma.frailty, model="iid",
    hyper = list(prec = list(initial=-5, fixed=TRUE)))
```

in the model formula is what indicates that the non-Gaussian components of the latent field are being approximated by a Gaussian with mean zero and low precision,  $\exp(-5)$  in this case. Please visit <http://www.r-inla.org/> for more information about the R package INLA.

```
# Simulate a dataset
#-----
n = 100 # number of groups
m = 10 # number of individuals in the same group
z = runif(n*m) # simulate covariate
eta = 1 + z # linear predictor
frailty = rgamma(n, 1, 1) # simulate frailties
y = rexp(n*m, rate = rep(frailty, each = m) * exp(eta)) # simulate data

# INLA code
#-----
## Construct an extended response vector Y.
yy = inla.surv(c(y, rep(NA, n)),
              c(rep(1, n*m), rep(NA, n))) # Observation component
ff = c(rep(NA, n*m), rep(1, n)) # Frailty component,
      # any observation will do, like '1'
Y = list(yy, ff) # extended response vector

## Construct extended covariates and frailties
intercept = c(rep(1, n*m), rep(NA, n)) # intercept
zz = c(z, rep(NA, n)) # covariate
loggamma.frailty = c(rep(1:n, each=m), 1:n) # frailty
## Model formula
formula = Y ~ -1 + intercept + zz +
          f(loggamma.frailty, model="iid",
            hyper = list(prec = list(initial=-5, fixed=TRUE)))
## prior for the frailty
hyper.frailty = list(prec = list(param=c(1, 1)))
```

```

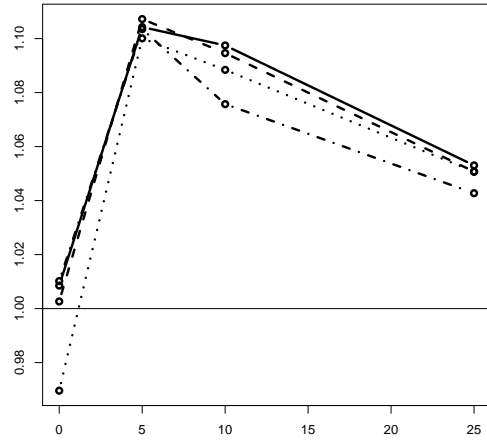
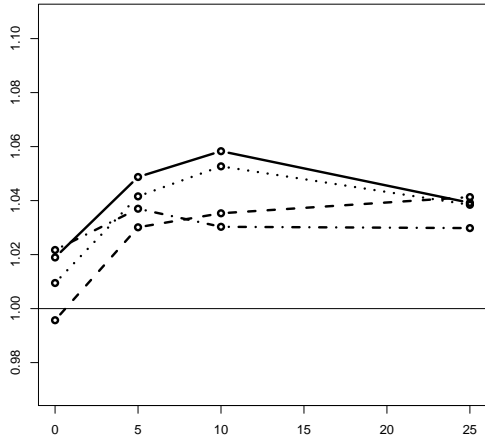
## Run inla function
rr = inla(formula,
          data = list(Y=Y, zz=zz, intercept=intercept,
                    loggamma.frailty= loggamma.frailty),
          family = c("exponential", "loggammafrailty"),
          control.data = list(list(), list(hyper = hyper.frailty)),
          control.fixed = list(prec = list(default = 0.01)),
          control.inla = list(strategy = "laplace")
          )

```

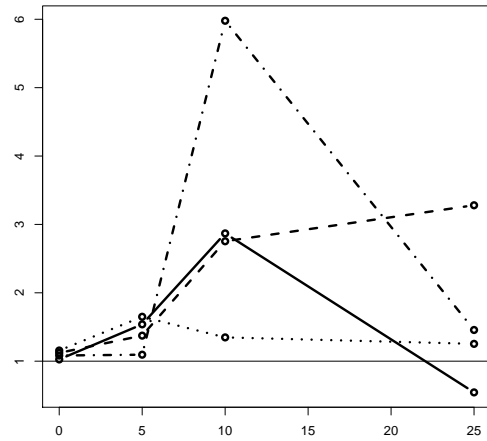
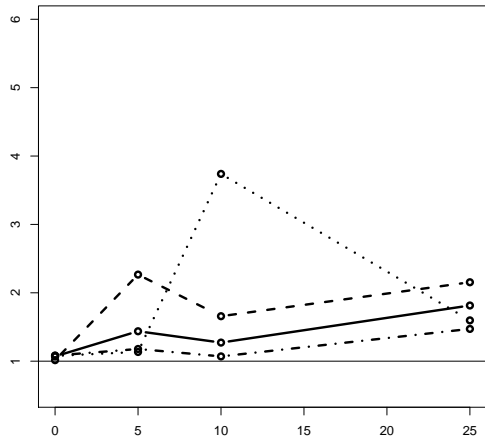
## References

- Box, G. (1980). Sampling and Bayes' inference in scientific modelling and robustness. *Journal of the Royal Statistical Society. Series A (General)*, 143(4):383–430.
- Conn, A. R., Gould, N. I., and Toint, P. L. (1987). *Trust region methods*, volume 1. Society for Industrial Mathematics.
- Gamerman, D. and Lopes, H. (2006). *Markov chain Monte Carlo: stochastic simulation for Bayesian inference*. Chapman & Hall/CRC.
- Ibrahim, J., Chen, M., and Sinha, D. (2001). *Bayesian survival analysis*. Springer.
- Kitagawa, G. (1987). Non-Gaussian state-space modeling of nonstationary time series. *Journal of the American statistical association*, 82(400):1032–1041.
- Laird, N. and Ware, J. (1982). Random-effects models for longitudinal data. *Biometrics*, pages 963–974.
- Lange, K., Little, R., and Taylor, J. (1989). Robust statistical modeling using the t distribution. *Journal of the American Statistical Association*, pages 881–896.
- Lunn, D., Spiegelhalter, D., Thomas, A., and Best, N. (2009). The bugs project: Evolution, critique and future directions. *Statistics in medicine*, 28(25):3049–3067.
- Martins, T. G., Simpson, D., Lindgren, F., and Rue, H. (2013). Bayesian computing with inla: new features.
- Pinheiro, J., Liu, C., and Wu, Y. (2001). Efficient algorithms for robust estimation in linear mixed-effects models using the multivariate t distribution. *Journal of Computational and Graphical Statistics*, 10(2):249–276.
- Robert, C. and Casella, G. (2004). *Monte Carlo statistical methods*. Springer Verlag.

- Rue, H. and Martino, S. (2007). Approximate Bayesian inference for hierarchical Gaussian Markov random field models. *Journal of statistical planning and inference*, 137(10):3177–3192.
- Rue, H., Martino, S., and Chopin, N. (2009). Approximate Bayesian inference for latent Gaussian models by using integrated nested Laplace approximations. *Journal of the Royal Statistical Society: Series B(Statistical Methodology)*, 71(2):319–392.
- Tierney, L. and Kadane, J. (1986). Accurate approximations for posterior moments and marginal densities. *Journal of the American Statistical Association*, pages 82–86.
- Vanhatalo, J., Jylänki, P., and Vehtari, A. (2009). Gaussian process regression with student-t likelihood. *Advances in Neural Information Processing Systems*, 22:1910–1918.



(a)  $\tau_e = 1/\sigma_e^2$  under close contamination pattern ( $f = 2$ ) (b)  $\tau_e = 1/\sigma_e^2$  under distant contamination pattern ( $f = 4$ )



(c)  $\tau_b = 1/\sigma_b^2$  under close contamination pattern ( $f = 2$ ) (d)  $\tau_b = 1/\sigma_b^2$  under distant contamination pattern ( $f = 4$ )

Figure 10: Relative efficiency (see Eq. (21)) of the  $t$  posterior mean with respect to the Gaussian posterior mean for the precision parameters in the linear mixed effect example. It plots the efficiency on the y-axis and  $p_e$  on the x-axis. The meaning for the different types of lines are: (Solid line)  $p_b = 0\%$ , (Dashed line)  $p_b = 5\%$ , (Dotted line)  $p_b = 10\%$  and (Dot-sash line)  $p_b = 25\%$ .